online data

Reactivity and endogenous modification by nitrite and hydrogen peroxide: does human neuroglobin act only as a scavenger?

Stefania NICOLIS*, Enrico MONZANI*, Chiara CIACCIO†, Paolo ASCENZI‡, Luc MOENS§ and Luigi CASELLA*[1]

*Dipartimento di Chimica Generale, Università di Pavia, Via Taramelli 12, 27100 Pavia, Italy, †Dipartimento di Medicina Sperimentale e Scienze Biochimiche, Università di Roma-Tor Vergata, Via Montpellier 1, 00133 Roma, Italy, ‡Dipartimento di Biologia, Università 'Roma Tre', Viale Guglielmo Marconi 446, 00146 Roma, Italy, and §Department of Biomedical Sciences, University of Antwerp, Universiteit 1, B-2610 Antwerp, Belgium

NGB (human neuroglobin), a recently discovered haem protein of the globin family containing a six-co-ordinated haem, is expressed in nervous tissue, but the physiological function of NGB is currently unknown. As well as playing a role in neuronal O_2 homoeostasis, NGB is thought to act as a scavenger of reactive species. In the present study, we report on the reactivity of metNGB (ferric-NGB), which accumulates *in vivo* as a result of the reaction of oxyNGB (oxygenated NGB) with NO, towards NO_2^- and H_2O_2. NO_2^- co-ordination of the haem group accounts for the activity of metNGB in the nitration of phenolic substrates. The two different metNGB forms, with and without the internal disulfide bond between Cys^{46} (seventh residue on the inter-helix region between helices C and D) and Cys^{55} (fifth residue on helix D), exhibit different reactivity, the former being more efficient in activating NO_2^-. The kinetics of the reactions, the NO_2^--binding studies and the analysis of the nitrated products from different substrates all support the hypothesis that metNGB is able to generate an active species with the chemical properties of peroxynitrite, at pathophysiological concentrations of NO_2^- and H_2O_2. Without external substrates, the targets of the reactive species generated by the metNGB/NO_2^-/H_2O_2 system are endogenous tyrosine (resulting in the production of 3-nitrotyrosine) and cysteine (oxidized to sulfinic acid and sulfonic acid) residues. These endogenous modifications were characterized by HPLC-MS/MS (tandem MS) analysis of metNGB after reaction with NO_2^- and H_2O_2 under various conditions. The internal S–S bond affects the functional properties of the protein. Therefore metNGB acts not only as scavenger of toxic species, but also as a target of the self-generated reactive species. Self-modification of the protein may be related to or inhibit its postulated neuroprotective activity.

Key words: cysteine oxidation, haem, human neuroglobin (NGB), oxidative stress, peroxynitrite, tyrosine nitration.

INTRODUCTION

NGB (human neuroglobin) was first identified in 2000 as a third globin-type protein, the other types of globins are Mb (myoglobin) and Hb [1]. NGB is expressed at low levels (in the micromolar range) in various regions of the brain, but at much higher levels ($\sim 100\ \mu$M) in retinal cells [1,2]. NGB is composed of 151 amino acids and has a high sequence similarity to mouse neuroglobin (94 % identity), but little homology with vertebrate Mbs and Hbs (< 21 % and < 25 % identity respectively) [1]. NGB differs from the other vertebrate globins in the binding of the six-co-ordinated haem group, with His^{96}[F8 (eighth residue on helix F)] and His^{64}(E7) acting as the fifth/proximal and sixth/distal ligands respectively, in both the ferrous and ferric forms of NGB [3,4] (Scheme 1). The presence of a six-co-ordinated haem reduces the affinity of the protein for ligands, with respect to the expected values, in the absence of competitive co-ordination by the distal histidine residue [3].

The function of NGB in the human brain remains unclear. In analogy with other globins, several possible physiological roles have been considered [5]. Indirect evidence suggests a role of NGB in neuronal O_2 homoeostasis, owing to the correlation between NGB expression and O_2 consumption [6]. The O_2 affinity of NGB depends on several factors, including the relative binding rates of O_2 with the haem sixth position and the competing distal histidine residue [3,7], and the redox state of the cell which controls the formation or cleavage of an internal disulfide bond between Cys^{46} [CD7 (seventh residue on the inter-helix region between helices C and D)] and Cys^{55}(D5) [8,9]. The presence of the S–S bond could perturb the three-dimensional structure of the CD–D (inter-helix region between helices C and D, extending to the end of helix D) region and affect the location of the neighbouring E-helix, thus modulating the binding of the endogenous His^{64}(E7) ligand to the haem group [9,10]. As a consequence, in ferrous NGB, the distal histidine residue dissociation rate increases by a factor of 10 with respect to the protein form without the disulfide bond [9,11], leading to an effective increase in O_2 affinity by the same factor [12] (Scheme 1).

O_2 storage or diffusion to or from the haem group of NGB may be assisted by the presence of a large protein matrix cavity (approx. 120 $Å^3$, where 1 Å = 0.1 nm), located between the haem distal site and the EF interhelical hinge and connected to the protein surface [10,13]. The cavity may be reshaped after ligand binding, which may allow trapping of harmful ROS (reactive oxygen species) or RNS (reactive nitrogen species) [14–17]. In particular, the increase in the concentration of NO up to the low

Abbreviations used: ABTS, 2,2′-azinobis-(3-ethylbenzothiazoline-6-sulfonic acid); CD, inter-helix region between helices C and D; CD7 etc., seventh residue on CD etc.; CID, collision-induced dissociation; DTT, dithiothreitol; EIC, extracted ion current; ESI, electrospray ionization; GdnHCl, guanidine hydrochloride; F8 etc., eighth residue on helix F etc.; NGB, human neuroglobin; h-NGB, modified NGB at high NO_2^- and H_2O_2 concentrations; h′-NGB_{SH}, modified NGB_{SH} at high H_2O_2 concentrations; HPA, 3-(4-hydroxyphenyl)propionic acid; LC, liquid chromatography; LPO, lactoperoxidase; lpo-NGB, modified NGB in the presence of LPO, NO_2^- and H_2O_2; Mb, myoglobin; hMb, human Mb; metNGB, ferric-NGB; NGB_{SH}, NGB without the internal disulfide bond; NGB_{S-S}, NGB with the internal disulfide bond; oxyNGB, oxygenated NGB; 4-PDS, 4,4′-dithiodipyridine; p-NGB, modified NGB at low NO_2^- and H_2O_2 concentrations; p′-NGB_{SH}, modified NGB_{SH} at low H_2O_2 concentrations; RNS, reactive nitrogen species; ROS, reactive oxygen species; TFA, trifluoroacetic acid.

[1] To whom correspondence should be addressed (email bioinorg@unipv.it).

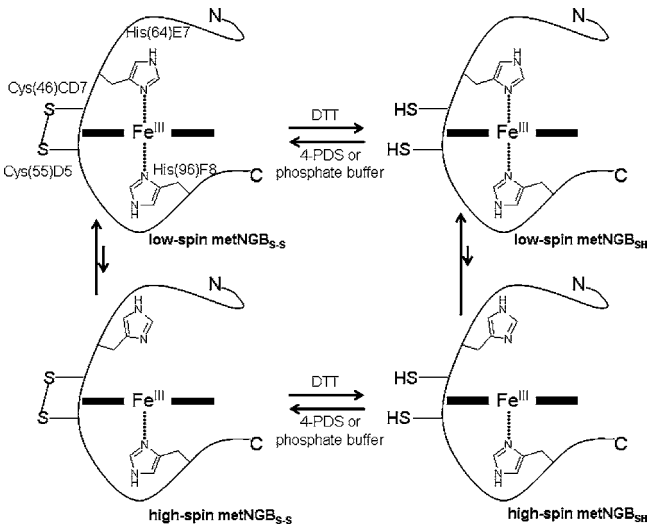

Scheme 1 Cysteine residue oxidation states and co-ordination equilibria in metNGB

Schematic representation of the low-spin/high-spin equilibria for metNGB$_{S-S}$ (left-hand side) and metNGB$_{SH}$ (right-hand side). The disposition of the side chains of the proximal and distal histidine residues [His^{96}(F8) and His^{64}(E7) respectively] is shown. The length of the vertical arrows indicates that, even if the co-ordination equilibrium is always shifted towards the six-co-ordinated species, in the case of metNGB$_{S-S}$, the amount of high-spin form is larger compared with metNGB$_{SH}$.

micromolar range, as observed under ischaemic conditions [18], may be contrasted with its reaction with oxyNGB (oxygenated NGB), yielding metNGB (ferric-NGB) and NO_3^- through a haem-bound $ONOO^-$ (peroxynitrite) intermediate [15]:

$$NGBFe^{II}O_2 + NO \rightarrow NGBFe^{III}OONO^- \rightarrow NGBFe^{III} + NO_3^- \quad (1)$$

As a metNGB reductase system has not yet been identified in the brain [15], the *in vivo* formation of metNGB through this mechanism may be physiologically relevant. Also, metNGB reacts with NO [19] to generate the stable $NGBFe^{II}NO$ species by reductive nitrosylation. This form of NGB is a good scavenger of $ONOO^-$, which oxidizes the protein back to metNGB as follows [19]:

$$NGBFe^{III} \xrightarrow{NO} NGBFe^{II}NO \quad (2)$$

$$NGBFe^{II}NO \xrightarrow{ONOO^-} NGBFe^{III}NO \quad (3)$$

$$NGBFe^{III}NO \longrightarrow NGBFe^{III} + NO \quad (4)$$

In contrast with Mb and Hb, the protein does not generate the ferryl form on reaction with H_2O_2 or $ONOO^-$ [20]. Also, no reaction was observed on the addition of NO_2^- [19].

Therefore even if the Fe^{III} centre of metNGB appeared to be protected by the co-ordinated distal histidine residue from attack by oxidizing species, the competitive co-ordination of exogenous ligands could account for the activation of alternative reactions. In the present study, we report on the reactivity of human metNGB in the presence of NO_2^- and H_2O_2, both of which are increased *in vivo* under conditions of oxidative stress [21]. The activation of NO_2^-/H_2O_2 by metNGB was assayed by the nitration of phenolic substrates [22–24] and an unexpectedly high reactivity was observed. Moreover, the two forms of the protein, metNGB$_{S-S}$ (NGB with the internal disulfide bond) and metNGB$_{SH}$ (NGB without the internal disulfide bond), are not equally as efficient in activating NO_2^- and H_2O_2. The issue of endogenous modification of metNGB, resulting from the reaction with NO_2^- and H_2O_2, at pathophysiological concentrations in the absence of external substrates was also addressed, since the identification of protein residues modified by ROS and RNS is essential for the understanding of the mechanisms involved in the development of various pathologies [25–29] and the postulated neuroprotective function of NGB. The endogenous targets of the reactive species generated by the protein are tyrosine and cysteine residues, and a more extensive pattern of modifications was observed for these residues than observed previously with hMb (human Mb) [24].

EXPERIMENTAL

Reagents

All buffer solutions were prepared using deionized Milli-Q water. ABTS [2,2′-azinobis-(3-ethylbenzothiazoline-6-sulfonic acid)], DTT (dithiothreitol), GdnHCl (guanidine hydrochloride), 30 % (v/v) H_2O_2 solution, HPA [3-(4-hydroxyphenyl)propionic acid], 4-hydroxybenzonitrile, 4-PDS (4,4′-dithiodipyridine), phenylacetic acid, sodium nitrite and trypsin were obtained from Sigma–Aldrich. All reagents were obtained at the best grade available. The concentration of H_2O_2 was controlled by monitoring the formation of the ABTS radical cation using a standard enzymatic method as published previously [30]. Recombinant human NGB was expressed and purified as reported previously [12]. In order to obtain a homogeneous sulfur-bridged form of NGB (i.e. NGB$_{S-S}$), the protein solution was dialysed overnight at 4 °C against 50 mM phosphate buffer, pH 7.5 (17 mM NaH_2PO_4 and 33 mM Na_2HPO_4). To reduce the intramolecular disulfide bond, forming NGB$_{SH}$, the NGB solution was dialysed at 37 °C against 1 mg/ml DTT dissolved in degassed 50 mM Tris/HCl, pH 7.5, and 0.5 mM EDTA under anaerobic conditions. After 30 min of dialysis, three exchanges of degassed 50 mM Tris/HCl, pH 7.5, and 0.5 mM EDTA were performed to eliminate DTT. Protein dialysis was carried out at 4 °C. In all of the experiments described below, when not explicitly stated, the proteins (NGB$_{S-S}$ and NGB$_{SH}$) were used in their ferric form. All spectrophotometric measurements were performed on a Hewlett Packard HP 8452A diode array spectrophotometer.

Kinetic studies of phenol nitration catalysed by NGB$_{S-S}$ and NGB$_{SH}$

The kinetic experiments were carried out in 200 mM phosphate buffer, pH 7.5 (68 mM NaH_2PO_4 and 132 mM Na_2HPO_4), using a quartz cuvette with a 1 cm-path-length, thermostated at 25.0 ± 0.1 °C and equipped with a magnetic stirrer. The initial solution, containing protein and variable substrate and NO_2^- concentrations in a final volume of 1.6 ml, was obtained by mixing solutions of the reagents (at an appropriate concentration) into the buffer. The reaction was started by the addition of H_2O_2 and was followed by monitoring A_{450} during the initial 10–15 s of the reaction. The conversion of the rate data from change in absorbance/s into [nitrophenol]/s was performed using the known molar absorption coefficient of HPA at 450 nm, $\varepsilon = 3350\ M^{-1} \cdot cm^{-1}$ [22]. The kinetic parameters were obtained from fitting of the plots of experimental rates at different substrate/NO_2^- concentrations to the appropriate equations.

For each substrate, the change in the reaction rate in the presence of various reactant concentrations was studied through a series of steps. First, a suitable concentration of H_2O_2 was found which would maximize the reaction rate, but avoided the use of excess oxidant. Secondly, this H_2O_2 concentration was used to study the dependence of the reaction rate on the

concentration of HPA, and, finally, the dependence of the reaction rate on the concentration of NO_2^- was examined. These steps were performed by following the iterative procedure described previously [23]. The concentration of NGB_{S-S} or NGB_{SH} used in these reactions was 1 μM, whereas the concentration of the other reactants for each of the steps is detailed as follows. Optimization of H_2O_2 concentration: using NGB_{S-S}, [HPA] = 1 mM, $[NO_2^-]$ = 0.3 M and $[H_2O_2]$ = 0.09–0.8 M; using NGB_{SH}, [HPA] = 0.4 mM, $[NO_2^-]$ = 1.0 M and $[H_2O_2]$ = 0.09–0.8 M. Dependence of the rate on varying HPA concentration: using NGB_{S-S}, $[H_2O_2]$ = 0.6 M, $[NO_2^-]$ = 0.3 M and [HPA] = 0.031–1.2 mM; using NGB_{SH}, $[H_2O_2]$ = 0.6 M, $[NO_2^-]$ = 1.0 M and [HPA] = 0.0096–0.96 mM. Dependence of the rate on varying the concentration of NO_2^-: using NGB_{S-S}, $[H_2O_2]$ = 0.6 M, [HPA] = 0.4 mM and $[NO_2^-]$ = 0.0062–0.44 M; using NGB_{SH}, $[H_2O_2]$ = 0.6 M, [HPA] = 0.3 mM and $[NO_2^-]$ = 0.037–2.5 M.

The reaction rates observed in the absence of the protein (non-catalytic reaction) or without H_2O_2 were completely negligible.

Binding of NO_2^-

In order to test the binding of NO_2^- to NGBs, a 1 cm-path-length quartz cuvette containing either 4.8 μM NGB_{S-S} or 5.2 μM NGB_{SH} in 200 mM phosphate buffer, pH 7.5, was incubated in increasing concentrations of NO_2^- in 200 mM phosphate buffer, pH 7.5 (final concentration from 0 to 0.42 M for NGB_{S-S} and from 0 to 0.64 M for NGB_S). The reaction was thermostatically controlled at 25.0 ± 0.1 °C, and UV–visible spectra were recorded after each increase in NO_2^- concentration. Blank spectra were recorded in the same way, but in the absence of protein. After subtracting the corresponding blank from each spectrum, the resulting spectra were corrected for dilution and then transformed into difference spectra by subtracting the native protein spectrum. A plot was constructed demonstrating the difference between A_{414} and A_{434} (these wavelengths had the maximum variation in difference spectra) against the ligand concentration.

For the binding of NO_2^- to NGB_{S-S}, the constants K_1 and K_2 were obtained by interpolation of the absorbance data with the binding isotherm for low-affinity binding of two consecutive ligands:

$$\Delta A = \left(\Delta A_{\infty 1} \times K_1 \times [NO_2^-]_{tot} + \Delta A_{\infty 2} \times K_1 \times K_2 \times [NO_2^-]_{tot}{}^2\right) / \left(1 + K_1 \times [NO_2^-]_{tot} + K_1 \times K_2 \times [NO_2^-]_{tot}{}^2\right)$$

where $\Delta A_{\infty 1}$ and $\Delta A_{\infty 2}$ represent the absorbance changes owing to the binding of one and two ligand molecules respectively, and $[NO_2^-]_{tot}$ is the total NO_2^- concentration, i.e. free plus bound NO_2^- concentrations. For the binding of NO_2^- to NGB_{SH}, the constant K_B was obtained by interpolation of the absorbance data with the binding isotherm for low-affinity binding of a single ligand:

$$\Delta A = \Delta A_\infty \times K_B \times [NO_2^-]_{tot} / (1 + K_B \times [NO_2^-]_{tot})$$

where ΔA_∞ represents the absorbance change as a result of binding NO_2^-, and $[NO_2^-]_{tot}$ is the total NO_2^- concentration.

HPLC analysis of the nitration products of 4-hydroxybenzonitrile and phenylacetic acid

The product mixtures derived from the nitration of 4-hydroxybenzonitrile and phenylacetic acid, promoted by the NGB/NO_2^-/H_2O_2 system, were analysed by HPLC using a Jasco MD-1510 instrument with diode array detection equipped with a Supelcosil™ LC18 reverse-phase semipreparative column (5 μm; 250 × 10 mm). Elution was carried out using 0.1 % TFA (trifluoroacetic acid) in distilled water (solvent A) and 0.1 % TFA in acetonitrile (solvent B), with a flow rate of 5 ml/min. Elution started with the use of 100 % solvent A for 5 min, followed by a linear gradient from 100 % solvent A to 100 % solvent B over 25 min. Spectrophotometric detection of the eluate was performed in the range of 200–600 nm.

The catalytic nitrations of 4-hydroxybenzonitrile and phenylacetic acid were studied under the following experimental conditions: $[NGB_{S-S}]$ = 1 μM, [substrate] = 1 mM, $[H_2O_2]$ = 0.6 M and $[NO_2^-]$ = 0.01, 0.05 or 0.15 M in 200 mM phosphate buffer, pH 7.5. The reaction mixtures were incubated for 10 min at room temperature (25 °C) and then were analysed by HPLC. The retention time of 4-hydroxybenzonitrile was 15.7 min, whereas the corresponding nitration product 4-hydroxy-3-nitrobenzonitrile was absent under all the conditions tested. Its retention time (17.4 min) was established using LPO (lactoperoxidase)-catalysed nitration, carried using the following conditions: [LPO] = 80 nM, [phenol] = 1 mM, $[H_2O_2]$ = 1 mM and $[NO_2^-]$ = 0.01 M in 200 mM phosphate buffer, pH 7.5. The HPLC chromatograms of the mixtures obtained from the nitration of phenylacetic acid showed there was unreacted substrate present at 16.8 min, two main peaks at 16.0 and 16.2 min, and two minor peaks at 14.5 and 14.7 min (obtained at both low and high NO_2^- concentrations).

HPLC analysis showed that no modification of 4-hydroxybenzonitrile and phenylacetic acid occurred in the absence of the protein. The presence of H_2O_2 was also demonstrated to be essential for the modification.

Modification of NGB in the presence of NO_2^- and H_2O_2

Samples of modified NGB_{S-S} and NGB_{SH} proteins were prepared by the addition of sodium nitrite and H_2O_2 to 60 μM NGB_{S-S} in 50 mM phosphate buffer, pH 7.5, or 60 μM NGB_{SH} in 50 mM Tris/HCl, pH 7.5, and 0.5 mM EDTA. Four different concentrations of sodium nitrite and H_2O_2 were added to create a variety of reaction conditions as follows: (i) pathophysiological conditions [21] (p-NGB_{S-S} and p-NGB_{SH}) of 0.1 mM NO_2^- and 0.15 mM H_2O_2 (divided into five aliquots of 30 μM each); (ii) harsh conditions [h-NGB_{S-S} (modified NGB at high NO_2^- and H_2O_2 concentrations) and h-NGB_{SH}] of 0.1 M NO_2^- and 1.0 mM H_2O_2 (divided into five aliquots); (iii) modifications without NO_2^- [p′-NGB_{SH} and h′-NGB_{SH} (modified NGB_{SH} at high H_2O_2 concentrations)] of 0.15 mM H_2O_2 (divided into five aliquots of 30 μM each) and 1.0 mM H_2O_2 (divided into five aliquots) respectively, and (iv) LPO-catalysed modifications [lpo-NGB_{S-S} (modified NGB in the presence of LPO, NO_2^- and H_2O_2) and lpo-NGB_{SH}] of 0.25 M NO_2^-, 0.15 mM H_2O_2 (divided into five aliquots) and 80 nM LPO.

The proteins were allowed to react at 20 °C for 10 min. Excess NO_2^- and oxidant were removed by overnight dialysis against 20 mM phosphate buffer, pH 7.5 (6.8 mM NaH_2PO_4 and 13.2 mM Na_2HPO_4) for NGB_{S-S} derivatives, and against degassed 20 mM Tris/HCl, pH 7.5, and 0.2 mM EDTA for NGB_{SH} derivatives.

Analysis of protein fragments and haem modification

For analysis of protein fragments, approx. 0.5 mg of unmodified NGB_{S-S} and NGB_{SH} and the derivatives p-NGB_{S-S}, h-NGB_{S-S}, lpo-NGB_{S-S}, p-NGB_{SH}, h-NGB_{SH}, p′-NGB_{SH}, h′-NGB_{SH} and lpo-NGB_{SH} was transformed into the apo protein using the standard HCl/2-butanone method [31] and was subsequently hydrolysed by trypsin. Digestion was performed using 1:50 (w/w) trypsin at

37 °C for 3 h in 20 mM ammonium bicarbonate solution, pH 8.0. Prior to HPLC-MS/MS analysis, the samples were incubated with 5 mM DTT for 15 min at 37 °C to prevent coupling of the cysteine-containing peptides during digestion. The reduction of the disulfide bonds was necessary for the quantification of unreacted cysteine residues in NGB derivatives.

Haem modification was studied by direct HPLC-MS/MS analysis of NGB derivatives in 20 mM ammonium bicarbonate solution, pH 8.0, after acidification with HCl to pH ~ 1.

LC (liquid chromatography)-MS and LC-MS/MS data were obtained using an LCQ ADV MAX ion-trap mass spectrometer equipped with an ESI (electrospray ionization) source and controlled by Xcalibur software 1.3 (Thermo Finnigan). ESI experiments were carried out in positive-ion mode under the following constant instrumental conditions: source voltage of 5.0 kV, capillary voltage of 46 V, capillary temperature of 210 °C and tube lens voltage of 55 V. The system was run in automated LC-MS/MS mode using a Surveyor HPLC system (Thermo Finnigan) equipped with a BioBasic™ C_{18} column (5 μm; 150 × 2.1 mm). The elution was performed using 0.1 % methanoic acid in distilled water (solvent A) and 0.1 % methanoic acid in acetonitrile (solvent B), at a flow rate of 0.2 ml/min. Elution started with 98 % solvent A for 5 min, followed by a linear gradient from 98 to 55 % solvent A in 65 min for the analysis of tryptic digests. A two-step linear gradient was used to analyse the non-digested protein solutions (98 to 50 % solvent A in 5 min, followed a gradient from 50 to 20 % solvent A in 40 min). MS/MS spectra obtained by CID (collision-induced dissociation) were performed with an isolation width of 2 *m*/*z*, the activation amplitude was approx. 35 % of the ejection RF (radio frequency) amplitude of the instrument.

For the analysis of protein fragments derived from NGB derivatives, the mass spectrometer was set such that one full MS scan was followed by a zoomscan and a MS/MS scan on the most intense ion observed from the MS spectrum. To identify the modified residues, the acquired MS/MS spectra were automatically searched against a protein database for NGB, using the SEQUEST® algorithm incorporated into Bioworks 3.1 (Thermo Finnigan).

GdnHCl denaturation assay

The denaturation stability of NGB_{SH}, p-NGB_{SH} and h-NGB_{SH} was determined by monitoring the absorbance variation of the Soret band of the protein (approx. 7 μM) after addition of increasing amounts of 8 M GdnHCl solution (up to 4.5 M final concentration) in degassed 50 mM Tris/HCl, pH 6.0, and 0.5 mM EDTA. Data were corrected for dilution caused by the addition of GdnHCl. The GdnHCl concentration at 50 % unfolding of the protein was evaluated from the curves of absorbance against denaturant concentration according to a standard method [32].

RESULTS

The two forms of NGB, with and without the disulfide bond

The purification of human NGB provides the protein in its ferric form, since oxyNGB was unstable *in vitro* and rapidly autoxidizes to metNGB ($t_{1/2}$ = 11 min) [7]. This was confirmed by the UV–visible spectrum characteristics of metNGB (Figure 1), as it was clearly distinguishable in the visible region from the spectrum of the Fe^{II}–O_2 form [for metNGB, λ_{max} = 532 nm, with a shoulder at 554 nm (Figure 1); for oxyNGB, λ_{max} = 543, 576 nm (results not shown)] [7,12]. The molar absorption coefficient of the Soret band of metNGB in the disulfide-bridged form (metNGB$_{S-S}$), obtained using the standard pyridine haemochrome assay [33] and used to determine protein concentration, was 1.29×10^5 $M^{-1} \cdot cm^{-1}$ at 414 nm (in 200 mM phosphate buffer, pH 7.5). The phosphate buffer used in our experiments is believed to promote the formation of disulfide bonds (Scheme 1) [12]. Actually, the number of accessible thiol groups per haem, as measured by the 4-PDS assay [12,34], was slightly lower than 1.0. This result is consistent with the presence of the single Cys^{120}(G19) in the reduced form and with the almost quantitative oxidation of the other two cysteines to a S–S bond [9]. These disulfide bonds are thought to play a significant role in the function of the protein [9,35].

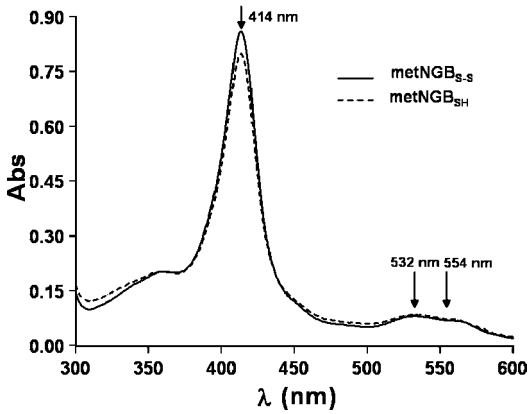

Figure 1 UV–visible spectra of metNGB$_{S-S}$ and NGB$_{SH}$

UV–visible spectra of 6.7 μM metNGB$_{S-S}$ (solid line) and 6.2 μM metNGB$_{SH}$ (dashed line) in 200 mM phosphate buffer, pH 7.5. The wavelength maxima are indicated (arrows).

Treatment of NGB_{S-S} with DTT under anaerobic conditions leads to the partial reduction of the disulfide bridge, as NGB_{SH} was stable to oxidation when kept in degassed 50 mM Tris/HCl, pH 7.5, and 0.5 mM EDTA at 4 °C. Different experimental conditions (temperature and reaction time) were examined to maximize the reduction of the S–S bond, with 2.4 cysteines per haem titrated in the protein observed after reaction with DTT for 30 min at 37 °C. It should be noted that the 4-PDS assay underestimates the number of thiol groups, since the initial fast reduction of 4-PDS to 4-thiopyridone by the SH groups of cysteine residues overlaps with the subsequent slow formation of the latter product by reaction with some reducing species that can be present in solution; therefore, it can be assumed that, in NGB_{SH}, almost all cysteine residues are in the reduced form.

The UV–visible spectra of the ferric forms of NGB_{S-S} and NGB_{SH} are identical (λ_{max} = 414 and 532 nm respectively, with a shoulder at 554 nm) and are characteristic of a six-co-ordinated ferric haem (Figure 1). Actually, even if the ratio between the high-spin and low-spin forms increased on formation of the disulfide bridge, the amount of the high-spin form would remain low (< 5 % at pH 7.5 [36] and < 10 % at pH 5 [37]). However, the only species detectable in the UV–visible spectra for both NGB_{S-S} and NGB_{SH} was the predominant six-co-ordinated species.

Lack of phenol oxidation by NGB

In the presence of H_2O_2, haem proteins such as Mb in their ferric form exhibit peroxidase-like activity towards phenolic substrates, oxidizing them to phenoxy radicals, which can give rise to dimer formation in solution [38,39]. The formation of these species can be followed spectrophotometrically through a characteristic absorption at a wavelength of approx. 300 nm. Moreover, a protein–ferryl intermediate (named compound II) can be detected in the

reactions of both Mb and peroxidases after addition of the oxidant. This was characterized by a red-shift of the protein Soret band from 408 to 424 nm for Mb [40], 403 to 420 nm for horseradish peroxidase [41] and 412 to 422 nm for LPO [42]. In contrast, no spectral change was observed after mixing of NGB (1 μM) with H_2O_2 (increasing concentrations up to 100 mM) in the absence or presence of a phenol, such as HPA. Indeed, Herold et al. [19] also reported that, in contrast with Mb and Hb, NGB does not generate the ferryl form of the protein, since its reactivity was strongly limited by the co-ordinated distal histidine residue. In fact, when NGB was reacted with H_2O_2 and HPA, the UV–visual spectrum features that are characteristic of phenolic dimers do not develop, indicating that the reactivity of NGB with H_2O_2 was negligible.

Phenol nitration is catalysed by NGB_{S-S} and NGB_{SH}

Surprisingly, NGB activates NO_2^- in the presence of H_2O_2, and this results in the nitration of the phenolic substrate HPA into the position *o*-relative to the hydroxy group. An analogous catalytic activity was reported for peroxidases [21,22,43,44] and the haem proteins Mb [23,24,45,46] and Hb [46]. The investigation of the kinetics of phenol nitration catalysed by NGB (both the NGB_{S-S} and NGB_{SH} forms) was not simple, since the reaction rate depends on the concentration of all the reagents. In order to gain an insight into the mechanism of nitration by the metNGB/NO_2^-/H_2O_2 system, it was necessary to investigate the reaction by varying the concentration of the reagents in a large range, far beyond the physiological concentrations likely to be encountered *in vivo*. Using the approximations and procedures followed previously for enzymatic nitration reactions [22], it was possible to obtain the kinetic parameters k_{cat} (the maximum turnover of the proteins), $K_M^{Ph\text{-}OH}$ (the dissociation constant of HPA from the complex formed with the proteins) and $k_{cat}/K_M^{Ph\text{-}OH}$ (used to calculate the dependence of the rate of reaction at low reagent concentrations on HPA) from the rate dependence on the HPA concentration, through the following equation:

$$\text{Rate} = \frac{k_{cat} \times [\text{NGB}] \times [\text{HPA}]}{K_M^{Ph\text{-}OH} + [\text{HPA}]} \quad (5)$$

and k_{cat}, $K_M^{nitrite}$ (the dissociation constant of NO_2^- from the complex formed with the proteins) and $k_{cat}/K_M^{nitrite}$ (used to calculate the dependence of the rate of reaction at low reagent concentrations on NO_2^-) from the rate dependence on NO_2^- concentration, through the following equation:

$$\text{Rate} = \frac{k_{cat} \times [\text{NGB}] \times [NO_2^-]}{K_M^{nitrite} + [NO_2^-]} \quad (6)$$

The data collected are displayed in Table 1, and the corresponding data for the nitration of HPA as catalysed by hMb [24] are also shown.

It is worth noting that the overall catalytic efficiency of NGB (expressed by k_{cat}, $k_{cat}/K_M^{Ph\text{-}OH}$ and $k_{cat}/K_M^{nitrite}$) was only slightly lower than that of Mb. This was surprising because the reactivity of the protein in the nitration reaction was expected to be negligible, owing to the presence of the six-co-ordinated haem group in NGB, as was observed for the phenol oxidation. Since the fraction of five-co-ordinated high-spin metNGB was less than 5% of total metNGB, its intrinsic reactivity must be very high, much greater than that of Mb. The interpretation of the kinetic parameters is complicated by the presence of the haem–distal histidine residue dissociation equilibrium, since the reported value of k_{-H} (rate constant for histidine residue release) of approx. 1 s^{-1} [36]) was of the same order of magnitude as the NGB k_{cat}. It follows that

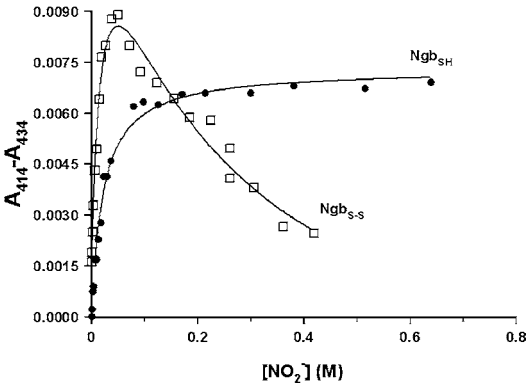

Figure 2 Binding of NO_2^- to NGB_{S-S} and NGB_{SH}

The difference between A_{414} and A_{434} in the UV–visible spectra of NGB_{S-S} (Ngb_{S-S}) and NGB_{SH} (Ngb_{SH}) after addition of NO_2^- compared with the ligand concentration is shown. The absorbance data were fitted with the binding isotherm for low-affinity binding of two ligands for NGB_{S-S}, and a single ligand for NGB_{SH}.

the high-spin/low-spin equilibrium is neither slow nor fast, so that, during the kinetic studies, a steady-state equilibrium was not reached in the initial phase and the predominant form of the protein that was present in solution tended to change with time.

The most interesting information emerged from the catalytic activity studied as a function of NO_2^- concentration, since the disulfide-bridged NGB_{S-S} exhibited a higher affinity for NO_2^- with respect to the thiol form NGB_{SH} ($K_M^{nitrite} = 43$ and 220 mM respectively). For ferrous NGB_{SH}, the distal histidine residue dissociation rate was nearly one order of magnitude smaller than that of NGB_{S-S}, thus leading to an effective decrease in O_2 affinity [9]. A similar effect of the S–S bond can be considered for the metNGBs on the iron affinity towards exogenous ligands such as NO_2^-. Therefore the larger $K_M^{nitrite}$ value observed for NGB_{SH} is in agreement with the requirement of NO_2^- co-ordination to the iron of NGB in order to promote nitrating activity.

The catalytic efficiency at low concentrations of NO_2^- (i.e. $k_{cat}/K_M^{nitrite}$) was similar for NGB_{S-S} and hMb, since the lower turnover rate of the former is compensated by its higher affinity for NO_2^-.

Binding of NO_2^- to NGB_{S-S} and NGB_{SH}

Small but significant changes can be observed in the spectrum of NGB_{S-S} in solution after the addition of excess NO_2^-. Difference spectra from optical titration clearly show both a smoothing and a slight shift towards higher energy of the Soret band during the first part of the binding process (NO_2^- concentration < 50 mM), and a slight decrease in the intensity of the band in the second part of the titration (NO_2^- concentration > 50 mM). The fitting of the changes in the Soret band as a function of NO_2^- concentration was consistent with low-affinity binding of two ligands, yielding the constants $K_1 = 51 \pm 15\ M^{-1}$ and $K_2 = 5 \pm 2\ M^{-1}$ (Figure 2). The former constant probably refers to the electrostatic interaction of an NO_2^- ion with the charged amino acid residues of the protein, and the latter constant to the co-ordination of an NO_2^- ion to the iron centre. As NO_2^- has to replace the distal histidine residue from the sixth co-ordination site, the affinity of NGB_{S-S} for NO_2^- results approx. one order of magnitude lower with respect to that previously obtained for hMb under the same conditions ($K_B = 76\ M^{-1}$) [24].

The NO_2^--binding experiment performed with NGB_{SH} showed a different behaviour with respect to NGB_{S-S}, since only the initial spectral changes were similar for the two proteins. Indeed, the data

Table 1 Kinetic data for HPA nitration catalysed by NGB and hMb

Steady-state kinetic parameters for NGB- and hMb-dependent HPA nitration by NO_2^-/H_2O_2 in 200 mM phosphate buffer, pH 7.5, at 25 °C.

Protein	$K_M^{Ph\text{-}OH}$ (mM)	k_{cat} (s^{-1})	$k_{cat}/K_M^{Ph\text{-}OH}$ ($M^{-1} \cdot s^{-1}$)	K_M^{Itrite} (M)	k_{cat} (s^{-1})	k_{cat}/K_M^{Itrite} ($M^{-1} \cdot s^{-1}$)
NGB_{S-S}	0.078 ± 0.008	0.177 ± 0.004	2300 ± 200	0.043 ± 0.006	0.140 ± 0.007	3.3 ± 0.3
NGB_{SH}	0.058 ± 0.008	0.132 ± 0.005	2300 ± 200	0.22 ± 0.03	0.139 ± 0.005	0.63 ± 0.06
hMb*	0.12 ± 0.02	0.67 ± 0.03	5600 ± 900	0.24 ± 0.04	1.03 ± 0.08	4.3 ± 0.5

* Data from [24].

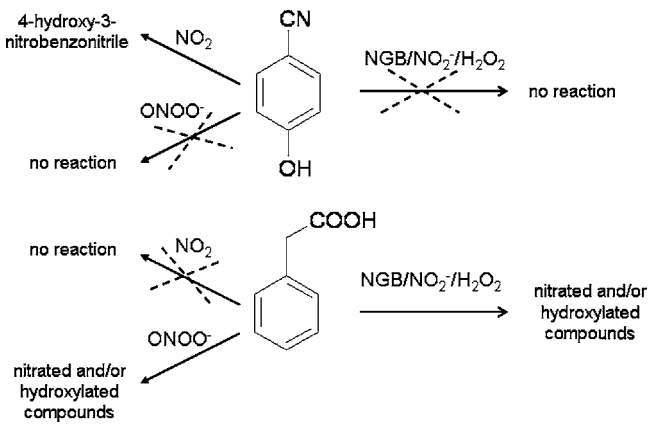

Scheme 2 Reactivity of 4-hydroxybenzonitrile and phenylacetic acid with RNS

Schematic representation of the reactivity of 4-hydroxybenzonitrile and phenylacetic acid with the nitrating agents NO_2 and $ONOO^-$, and the catalytic system metNGB/NO_2^-/H_2O_2.

could be fitted with a single binding isotherm, giving the association constant $K_B = 48 \pm 5\ M^{-1}$, which was very similar to the K_1 value obtained with NGB_{S-S} (Figure 2). By analogy, the process can be associated with the electrostatic interaction of NO_2^- to NGB_{SH}. It was impossible to obtain a reliable binding constant for the direct co-ordination of NO_2^- to the haem iron for NGB_{SH}, thus confirming the lower affinity of the thiol form of the protein for exogenous ligands with respect to the disulfide-bridged NGB, as was also observed from the kinetic studies of phenol nitration.

The interaction of NGB with NO_2^- was also investigated by Herold et al. [19], but, at the low NO_2^- concentration employed (< 1 mM), the binding of NO_2^- was not observed. Since metNGB was active in promoting the nitration reaction at low concentrations of NO_2^- (pathophysiological values), a small and hardly detectable fraction of the haem iron must be accessible to the ligand.

Nitration of 4-hydroxybenzonitrile and phenylacetic acid

The substrates phenylacetic acid and 4-hydroxybenzonitrile were used as mechanistic probes for the nitration reaction catalysed by NGB/NO_2^-/H_2O_2. The reaction could proceed through the formation of the same nitrating species involved in the reactions promoted by peroxidases and Mb, i.e. nitrogen dioxide (NO_2) or $ONOO^-$, depending on the NO_2^- concentration [22–24]. Phenylacetic acid reacts with $ONOO^-$, generating nitrated and/or hydroxylated compounds, but it is unreactive to NO_2 and thus it is a good probe for $ONOO^-$. The reactivity of 4-hydroxybenzonitrile is different, since it reacts with NO_2 to generate 4-hydroxy-3-nitrobenzonitrile, whereas $ONOO^-$ is a poor nitrating agent for this substrate [22] (Scheme 2).

4-Hydroxybenzonitrile was reacted with NGB and H_2O_2 at different NO_2^- concentrations (10–150 mM) and the reaction mixtures were analysed by HPLC. The nitrated product was absent under all of the conditions tested, indicating that NO_2 was not formed, or was formed in negligible amounts, by NGB under these conditions. In contrast, NGB/NO_2^-/H_2O_2 induced the modification of phenylacetic acid, and by HPLC it was possible to separate four different products, regardless of the NO_2^- concentration used. These derivatives shared spectral features and retention times with the products obtained in the reaction of phenylacetic acid with $ONOO^-$ [22]. These results suggest that the nitration catalysed by NGB in the presence of NO_2^- and H_2O_2 proceeds through the formation of a reactive species with the chemical properties of $ONOO^-$ (Scheme 2).

Tandem MS/MS analysis of NGB_{S-S} and NGB_{SH} modified by H_2O_2 and NO_2^-

To investigate the endogenous modifications undergone by NGB in the presence of NO_2^- and H_2O_2, NGB (both in the NGB_{S-S} and NGB_{SH} forms) was reacted with varying quantities of NO_2^- and H_2O_2 in the absence of an external substrate. Depending on the concentration of the reagents used, a series of protein derivatives was prepared under very mild conditions (similar to those that can occur under pathophysiological conditions [21]), and NGB_{S-S} and NGB_{SH} were reacted with 0.1 mM NO_2^- and 0.15 mM H_2O_2, obtaining p-NGB_{S-S} and p-NGB_{SH} respectively. Using less physiological and more harsh conditions, NGB_{S-S} and NGB_{SH} were reacted with 100 mM NO_2^- and 1 mM H_2O_2, obtaining h-NGB_{S-S} and h-NGB_{SH} respectively. The reactivity of the cysteine residues in the presence of H_2O_2 alone was studied by reacting NGB_{SH} with H_2O_2 at low (0.15 mM) and high (1 mM) oxidant concentrations, obtaining p′-NGB_{SH} and h′-NGB_{SH} respectively.

Moreover, generation of the NGB derivatives by NO_2^- and H_2O_2 was performed in the presence of LPO, as an external source of the nitrating agent. The protein derivatives obtained under these conditions were named as lpo-NGB_{S-S} and lpo-NGB_{SH}.

The UV–visible spectra of the p-NGB derivatives were indistinguishable from that of native metNGB, whereas the spectra for the h-NGB and lpo-NGB derivatives both exhibited a slight broadening of the Soret band and the appearance of a shoulder at approx. 440–450 nm was also observed. These spectral features were associated with haem nitration and reflected the colour change of the protein solutions from brown to greenish-brown, which accompanied the formation of h-NGB_{S-S}, h-NGB_{SH}, lpo-NGB_{S-S} and lpo-NGB_{SH} derivatives [24]. All of the protein derivatives were analysed by HPLC-ESI-MS/MS, with the aim of investigating the endogenous modifications and the results are shown in Tables 2 and 3. The potential targets of the oxidizing and nitrating species are, besides the haem prosthetic group, the

Table 2 Haem and tyrosine residue modifications in NGB derivatives

Nitration of haem and tyrosine residues in NGB derivatives obtained under the following conditions: for p-NGBs, [NGB] = 60 μM, [NO_2^-] = 0.1 mM and [H_2O_2] = 0.15 mM; for h-NGBs, [NGB] = 60 μM, [NO_2^-] = 0.1 M and [H_2O_2] = 1 mM; for lpo-NGBs, [LPO] = 80 nM, [NGB] = 60 μM, [NO_2^-] = 0.25 M and [H_2O_2] = 0.15 mM. All reactions were performed in 200 mM phosphate buffer, pH 7.5.

Protein derivatives	Nitration (%)				
	Haem-NO_2	Tyr^{44}-NO_2	Tyr^{88}-NO_2	Tyr^{115}-NO_2	Tyr^{137}-NO_2
p-NGB_{S-S}	0	0	0.6	0	0
p-NGB_{SH}	0	0	1	0	0
h-NGB_{S-S}	38	50	11	65	38
h-NGB_{SH}	14	11	7	36	14
lpo-NGB_{S-S}	25	5	1.3	3.5	15
lpo-NGB_{SH}	27	2.3	0.9	7	11

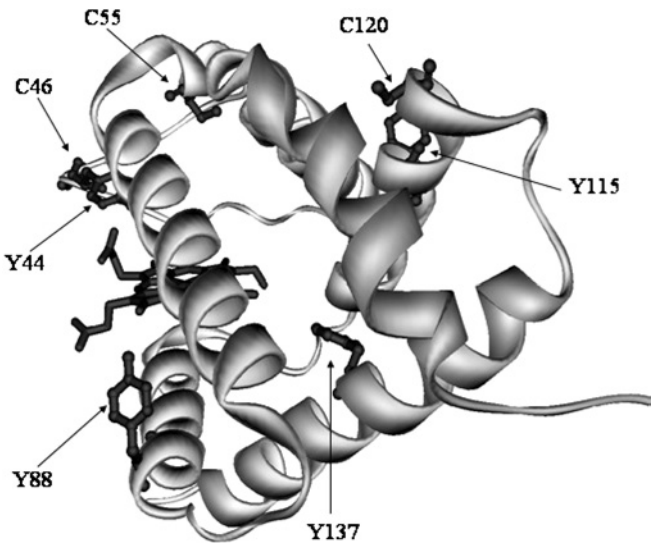

Figure 3 Structure of NGB

Structure of the C46G/C55S/C120S mutant of NGB. The atomic co-ordinates were obtained from [10] and the Protein Data Bank (accession number 1OJ6). The disposition of the side chains of the tyrosine residues (Tyr^{44}, Tyr^{88}, Tyr^{115} and Tyr^{137}), and the cysteine residues (Cys^{46}, Cys^{55}, and Cys^{120}) present in the wild-type protein are shown.

protein tyrosine residues Tyr^{44}(CD3), Tyr^{88} (F3), Tyr^{115}(G14) and Tyr^{137}(H12), and the cysteine residues Cys^{46}(CD7), Cys^{55}(D5) and Cys^{120}(G19) in NGB_{SH}, with Cys^{120}(G19) being the only cysteine residue target in NGB_{S-S} (Figure 3).

The modification of the prosthetic group can be detected by direct HPLC-MS/MS analysis of the acidified protein solution, since the haem group was released from the protein. The modified haemin was detected only in the NGB derivatives obtained after reaction with high levels of NO_2^- and H_2O_2, i.e. h-NGB_{S-S} and h-NGB_{SH}. In particular, ions with *m*/*z* 616 and 661 were identified, corresponding to free haemin and haemin modified with a NO_2 group [23,24] respectively. The modification probably occurs at one of the haem vinyl groups, in analogy with the haem nitration observed after treatment of Mb with a large excess of NO_2^- at pH 5.5 [47]. Integration of the peaks in the EIC (extracted ion current) chromatograms indicated that haemin nitration occurred with a 38 % yield in h-NGB_{S-S}, a 14 % yield in h-NGB_{SH}, a 25 % yield in lpo-NGB_{S-S} and a 27 % yield in lpo-NGB_{SH} (Table 2).

The modifications at the cysteine and tyrosine residues were characterized on polypeptide fragments resulting from tryptic digestion of the apoNGB derivatives. The HPLC-ESI-MS/MS analysis showed the presence of many modified peptide fragments (for the molecular masses and *m*/*z* values as bicharged ions, see Supplementary Table S1 at http://www.BiochemJ.org/bj/407/bj4070089add.htm). The analysis of the MS/MS spectra using the SEQUEST® algorithm allowed the assignment of the modifications to the nitration of the tyrosine residues to 3-nitrotyrosine [23] and the oxidation of the cysteine residues to sulfinic (R-SO_2H) and sulfonic (R-SO_3H) acids. As an example of the MS results, the MS/MS spectrum of the peptide from amino acid residue 68 to 94, obtained by the analysis of h-NGB_{S-S} (nitrated at Tyr^{88}), is shown in Figure 4.

The percentage of residue modifications is shown in Tables 2 and 3, and was obtained by comparing the areas of the peaks in the EIC chromatograms that corresponded to the derivatized peptides with those of the corresponding peptides in the starting proteins. The greater efficiency of NGB_{S-S}, in promoting self-nitration of both the haem group and the tyrosine residues by NO_2^- and H_2O_2, compared with NGB_{SH} was clearly apparent from the amount of endogenous modifications observed for h-NGB_{S-S} and h-NGB_{SH} (Table 2). This is in agreement with the kinetic parameters for phenol nitration (Table 1), since NGB_{S-S} exhibits a significantly higher catalytic efficiency in terms of $k_{cat}/K_M^{nitrite}$ compared with NGB_{SH}.

A complete picture of the cysteine residue derivative formation is provided by the modification of NGB_{SH} under different conditions, resulting in the formation of the h-, p-, h′- and p′-NGB_{SH} derivatives (Table 3). All of the cysteine residues were oxidized to sulfinic and sulfonic acids and the amount of modification induced by NO_2^- and H_2O_2 increased with the concentration of the reagents (compare p-NGB_{SH} with h-NGB_{SH}), and was significantly lower in the absence of NO_2^- (h′-NGB_{SH} compared with p′-NGB_{SH}), indicating that the NGB/NO_2^-/H_2O_2 system generates distinctive oxidant species.

The mechanism of protein modification was explored by inducing the formation of the NGB derivatives in the presence of an external catalyst. The enzyme LPO was chosen, since it reacts with H_2O_2 and NO_2^- to generate nitrating species with a rate two orders of magnitude larger when compared with NGB [22]. Thus when NGB reacted with NO_2^- at low H_2O_2 concentration and in the presence of LPO, the reactive species were generated by the enzyme, making NGB self-promoted derivative formation negligible. This was confirmed by the similarity in the extent of nitration (both at the haem group and the tyrosine residues) obtained for the LPO-promoted modification of NGB_{S-S} and NGB_{SH} (Table 2).

From the analysis of the derivatives lpo-NGB_{S-S} and lpo-NGB_{SH}, it emerged that the IPO-promoted NGB tyrosine residue nitration and cysteine residue oxidation occurred to a lower extent compared with the modifications which are self-promoted by NGB. In contrast, the haem group was the favoured modification site for both lpo-NGBs (Tables 2 and 3). These results indicated that the prosthetic group was the most accessible target for the LPO-generated reactive species, whereas the NGB-generated reactive species exhibited a preference for intramolecular, rather than intermolecular, reactivity.

GdnHCl denaturation assay

The unfolding midpoint [D_0] in the presence of GdnHCl for NGB_{SH}, p-NGB_{SH} and h-NGB_{SH} was estimated to be in the range of 4.1–4.2 M, as obtained from the curves of absorbance against denaturant concentration. These values can be compared with those obtained under the same conditions for sperm whale Mb ([D_0] = 1.46 M [32]), and horse heart Mb ([D_0] = 1.32 M)

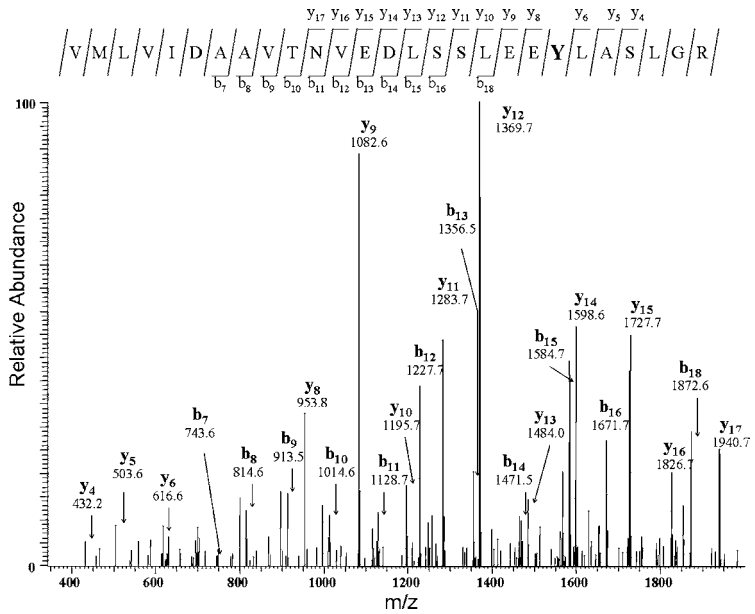

Figure 4 CID spectrum of the modified amino acid 68–94 peptide

MS/MS spectrum of the *m*/*z* 1477.6 peak (mass of 2953.3 Da) assigned to the amino acid 68–94 peptide in a double-charged state and with Tyr^{88} modified to 3-nitrotyrosine. The assignment of the *y* and *b* ion series is shown. Above the spectrum, the sequence of the 68–94 peptide, with the modified residue in bold, and the summary of the *y* and *b* ions found in the spectrum is shown.

Table 3 Modification of cysteine residues in NGB derivatives

Oxidation of cysteine residues in NGB derivatives obtained by protein modification under the following conditions: for p-NGBs, [NGB] = 60 μM, [NO_2^-] = 0.1 mM and [H_2O_2] = 0.15 mM; for h-NGBs, [NGB] = 60 μM, [NO_2^-] = 0.1 M and [H_2O_2] = 1 mM; for lpo-NGBs, [LPO] = 80 nM, [NGB] = 60 μM, [NO_2^-] = 0.25 M and [H_2O_2] = 0.15 mM; for p′-NGB_{SH}, [NGB] = 60 μM and [H_2O_2] = 0.15 mM; for h′-NGBs, [NGB] = 60 μM and [H_2O_2] = 1 mM. All reactions were performed in 200 mM phosphate buffer, pH 7.5.

	Oxidation (%)					
Protein derivatives	Cys^{46}-SO_2H	Cys^{46}-SO_3H	Cys^{55}-SO_2H	Cys^{55}-SO_3H	Cys^{120}-SO_2H	Cys^{120}-SO_3H
NGB_{S-S}	*	*	*	*	1.7	1.5
NGB_{SH}	0.3	0.9	0.6	1.7	2	2
p-NGB_{S-S}	*	*	*	*	2	2
p-NGB_{SH}	2.3	4.5	2.5	7	10	9
p′-NGB_{SH}	1	2	0.5	2	2	1.5
h-NGB_{S-S}	*	*	*	*	5	8
h-NGB_{SH}	21	14	4	14	18	16
h′-NGB_{SH}	0.9	4	0.7	4	5	6
lpo-NGB_{S-S}	*	*	*	*	6	7
lpo-NGB_{SH}	22	8	3	7	10	5

* Cys^{46} and Cys^{55} are involved in the S–S bond.

(E. Monzani, S. Nicolis, R. Roncone, M. Barbieri, A. Granata and L. Casella, unpublished work). Therefore NGB exhibited a considerably higher stability to GdnHCl than Mbs. Moreover, the derivatization of the protein residues (nitration of tyrosine residues and oxidation of cysteine residues) in the h-NGB_{SH} derivative had very little effect on the stability of the protein. Treatment of NGB with pathophysiological NO_2^- and H_2O_2 concentrations, yielding p-NGB_{SH}, induced completely negligible effects on protein stability to GdnHCl denaturation. A similar negligible effect towards denaturation was observed for horse heart Mb after nitration of tyrosine residues in the presence of NO_2^- and H_2O_2 ([D_0] = 1.35 M compared with 1.32 M for native Mb). A more detailed characterization of the unfolding properties of NGB and its derivatives will be carried out separately.

DISCUSSION

In vivo NGB species

Since NGB possesses a bis-histidine six-co-ordinated haem group, the reactivity of the protein towards exogenous ligands is regulated by the dissociation rate of the distal histidine residue. Nevertheless, NGB in its ferrous state has significant reactivity towards small ligands, such as NO, O_2 and CO (carbon monoxide). The competition between these external molecules and the histidine residue for the sixth co-ordination site of the Fe^{II} centre emerges from the kinetic and thermodynamic constants previously reported [3,4,48]. It follows that, in spite of the high intrinsic affinity of NGB for both O_2 and CO, the binding of these ligands is suggested to be slow *in vivo* [7]. Furthermore, the

influence of the internal disulfide bridge on the affinity of ferrous NGB_{S-S} for molecular O_2 has been clearly demonstrated [9].

In the reducing conditions that exist within living cells, NGB would be present in the ferrous NGB_{SH} form, saturated with O_2 at approx. 12 % [12]. Although the ferric form studied in the present paper may not be the most physiologically relevant form of the protein, the presence of H_2O_2 and NO_2^- would rapidly convert ferrous or oxyNGB into the ferric form. Furthermore, metNGB is the product of rapid NO scavenging by oxyNGB, so, in the absence of a metNGB reductase, a system would accumulate metNGB (according to reaction 1) [15].

MetNGB promoted nitration of phenolic compounds

Currently, the only data concerning the behaviour of metNGB with H_2O_2 indicated an absence of reactivity [19]. The results reported in the present study show an interesting pseudo-enzymatic activity of metNGB in the presence of H_2O_2 and NO_2^-. Even if the mechanism of the NGB reaction could be considered to be similar to that of peroxidases, this is in contrast with the absence of activity of metNGB in the oxidation of phenolic compounds observed in the presence of H_2O_2 alone. In fact, under these conditions, metNGB does not generate the ferryl species compounds I and II, which are the characteristic intermediates of the catalytic cycle of peroxidases. Nevertheless, in analogy with peroxidases, metNGB promotes the nitration of phenolic substrates by activation of NO_2^- and H_2O_2. This result is not in contradiction with the absence of the reaction observed between NGB and H_2O_2, since, besides the peroxidase-like mechanism of nitration through NO_2, an alternative mechanism for the nitration of phenolic substrates emerged in our previous studies on peroxidases and Mb in the presence of NO_2^- and H_2O_2 [22,23]. This mechanism involved the initial binding of NO_2^- to the haem iron, followed by the reaction of H_2O_2 with the co-ordinated NO_2^-, to produce an iron-bound $ONOO^-$ [$NGBFe^{III}$-N(O)OO], which acts as the nitrating active species. In the case of peroxidases and Mbs, the $ONOO^-$ pathway becomes important only at relatively high NO_2^- concentrations [22–24], whereas with NGB it is demonstrated that this is the only mechanism active in the nitration of exogenous and endogenous phenolic groups (i.e. tyrosine residues) even in the pathophysiological concentration range of NO_2^- and H_2O_2 (Scheme 3).

The $ONOO^-$ pathway

The kinetic parameters for HPA nitration reported in Table 1 show the importance of NO_2^- in discriminating the reactivity of $metNGB_{S-S}$ and $metNGB_{SH}$. As expected from the influence of the internal S–S bond on the binding rate of exogenous ligands to the iron centre, the kinetic parameters for the two forms of the protein and their dependence on NO_2^- concentration are significantly different, supporting the hypothesis of direct co-ordination of NO_2^- to the Fe^{III} centre to promote catalysis. In particular, $metNGB_{S-S}$ exhibits larger values, both for NO_2^- affinity [extrapolated from kinetic data ($1/K_M^{nitrite}$)] and for reactivity at low NO_2^- concentrations ($k_{cat}/K_M^{nitrite}$) with respect to $metNGB_{SH}$, indicating that the interaction of NO_2^- with the catalytic site regulates the efficiency of nitration at low concentrations of the reagent, in conditions that can occur *in vivo*. The higher affinity of NO_2^- for $metNGB_{S-S}$ compared with $metNGB_{SH}$ was confirmed by NO_2^--binding studies (Figure 2).

The $ONOO^-$ pathway proposed for the nitrating activity of metNGB was examined by the observation of the reaction with 4-hydroxybenzonitrile and phenylacetic acid, which are mechanistic probes of NO_2 and $ONOO^-$ respectively. The lack of reactivity of hydroxybenzonitrile on one hand, and the presence of several products deriving from nitration and/or hydroxylation of phenylacetic acid on the other hand, is in agreement with the formation of an active species with the chemical properties of $ONOO^-$ by metNGB (Scheme 2). It follows that the formation of a protein-bound $ONOO^-$ intermediate is a reasonable step for nitration catalysed by metNGB in the presence of NO_2^- and H_2O_2, even at rather low concentrations of the reagents.

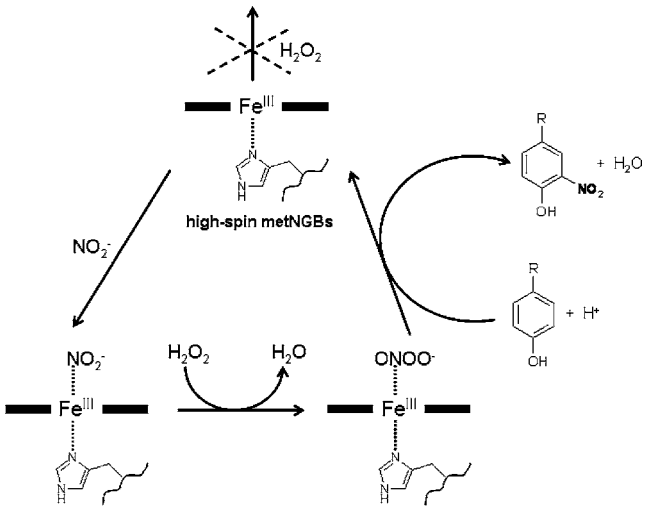

Scheme 3 Mechanism of metNGB promoted nitration of phenolic compounds

Schematic representation of the activation of NO_2^- and H_2O_2 by the high-spin metNGBs ($metNGB_{S-S}$ or $metNGB_{SH}$) through the $ONOO^-$ pathway, involving the initial binding of NO_2^- to the haem iron, followed by the reaction with H_2O_2, to produce an iron-bound $ONOO^-$ ($NGBFe^{III}$-N(O)OO) nitrating active species. Nitration of phenol occurs at the *o*-position relative to its hydroxy group. The upper part of the scheme shows the absence of reactivity of metNGB with H_2O_2.

NGB endogenous modifications

The generation and activity of the oxidant species formed by metNGB was examined by identification of the pattern of protein modifications obtained using LPO as an external catalyst, in comparison with metNGB-promoted endogenous modifications (Tables 2 and 3). At the high NO_2^- concentration (250 mM) used for the preparation of lpo-NGB_{S-S} and lpo-NGB_{SH} derivatives, LPO-promoted nitration proceeded through the formation of the $ONOO^-$ active species [22]. The differences in the pattern of residues modified by the LPO-generated $ONOO^-$ in comparison with those self-induced by NGB indicated that, in the latter case, $ONOO^-$ reacts intramolecularly. Moreover, the $ONOO^-$ reactive species are probably responsible for the oxidation of cysteine residues to form the corresponding sulfinic and sulfonic acids. Not only can it promote this type of modifications, as observed in the oxidations of BSA and hMb [24,49], but the high reactivity of this species also accounts for the lower extent of derivatization observed in the h′-NGB_{SH} and p′-NGB_{SH} derivatives (obtained by reaction with H_2O_2 only) in comparison with the h-NGB_{SH} and p-NGB_{SH} derivatives respectively. The less physiological conditions used in the preparation of the h-NGB_{SH} and h-NGB_{S-S} derivatives, which forced the extent of endogenous modifications, allowed the investigation of the competitive reactivity of the protein residues. Both the presence of three reactive cysteine residues (which may scavenge RNS) in NGB_{SH}, and its poorer catalytic efficiency in the nitration of phenolic compounds compared with NGB_{S-S}, may account for the lower degree of tyrosine residue nitration in h-NGB_{SH}.

From the point of view of the physiological relevance of NGB endogenous modifications, the analysis of p-NGB_{SH} was of particular interest, since this form was obtained from NGB_{SH} (presumed to be the predominant form *in vivo* [12]) with low concentrations of NO_2^- and H_2O_2. Among the protein residues, cysteine residues had the highest reactivity towards the $ONOO^-$ active species, and their reaction prevented nitration of tyrosine residues and the haem prosthetic group. It is possible to calculate that approx. 36 % of H_2O_2-oxidizing equivalents introduced were used for oxidation of cysteine residues to sulfinic and sulfonic acids. Oxidation of cysteine residues to sulfinic and sulfonic acid derivatives has been observed [50,51], together with other types of oxidations that can be reversed by reaction with biological thiols [52]. It is worth noting that, among the tyrosine residues, the only one that undergoes nitration in both p-NGB_{S-S} and p-NGB_{SH} is Tyr^{88}, the phenolic hydroxy group of which points toward the large NGB cavity connected to the haem distal site [10]. This may indicate that the $ONOO^-$ reactive species endogenously generated at the haem distal site can easily diffuse through the cavity and nitrate Tyr^{88}.

Does human NGB act only as a scavenger?

In the globins, cysteine residues often play specific roles, and this is modulated by the formation of intramolecular or intermolecular disulfide bonds [9]. In the case of NGB, the oxidation state of Cys^{46} and Cys^{55} is relevant because it is linked to the peculiar six-co-ordination of the haem. The present study confirms the importance of the internal S–S bond in controlling the reactivity of metNGB towards NO_2^- and H_2O_2. It also shows that the protein can be involved in other activities. NGB is thought to act as a scavenger of toxic species generated *in vivo* under conditions of oxidative stress. But the ability of the metNGB form generated by this activity to activate NO_2^- and H_2O_2 means that, besides acting as a scavenger, NGB can be the source of RNS, thus affecting its physiological activity. A significant fraction of the nitrating and oxidizing species (approx. 36 % in the conditions used to prepare p-NGB_{SH}) does not escape from the protein, but is consumed in the self-modification of NGB. The easy oxidation of cysteine residues to sulfinic and sulfonic acids may be one way used by NGB to scavenge part of the generated RNS. To gain a better understanding of the physiological relevance of these reactions, it will be important to analyse the state of endogenous modification of samples of the protein isolated after *in vivo* exposure to oxidative stress conditions.

This work was supported by funds from PRIN (Progetto di Ricerca di Interesse Nazionale) and FIRB (Fondo per gli Investimenti della Ricerca di Base) projects of the Italian MIUR (Ministero dell'Istruzione, dell'Università e della Ricerca Scientifica). The University of Pavia, the European COST D21 Action and CIRCMSB (Consorzio Interuniversitario di Ricerca in Chimica dei Metalli nei Sistemi Biologici) are also gratefully acknowledged for support.

REFERENCES

1 Burmester, T., Weich, B., Reinhardt, S. and Hankeln, T. (2000) A vertebrate globin expressed in the brain. Nature **407**, 520–523
2 Schmidt, M., Giessl, A., Laufs, T., Hankeln, T., Wolfrum, U. and Burmester, T. (2003) How does the eye breathe? Evidence for neuroglobin-mediated oxygen supply in the mammalian retina. J. Biol. Chem. **278**, 1932–1935
3 Trent, III, J. T., Watts, R. A. and Hargrove, M. S. (2001) Human neuroglobin, a hexacoordinate hemoglobin that reversibly binds oxygen. J. Biol. Chem. **276**, 30106–30110
4 Uno, T., Ryu, D., Tsutsumi, H., Tomisugi, Y., Ishikawa, Y., Wilkinson, A. J., Sato, H. and Hayashi, T. (2004) Residues in the distal heme pocket of neuroglobin. Implications for the multiple ligand binding steps. J. Biol. Chem. **279**, 5886–5893
5 Hankeln, T., Ebner, B., Fuchs, C., Gerlach, F., Haberkamp, M., Laufs, T. L., Roesner, A., Schmidt, M., Weich, B., Wystub, S. et al. (2005) Neuroglobin and cytoglobin in search of their role in the vertebrate globin family. J. Inorg. Biochem. **99**, 110–119
6 Garry, D. J. and Mammen, P. P. A. (2003) Neuroprotection and the role of neuroglobin. Lancet **362**, 342–343
7 Dewilde, S., Kiger, L., Burmester, T., Hankeln, T., Baudin-Creuza, V., Aerts, T., Marden, M. C., Caubergs, R. and Moens, L. (2001) Biochemical characterization and ligand binding properties of neuroglobin, a novel member of the globin family. J. Biol. Chem. **276**, 38949–38955
8 Hamdane, D., Kiger, L., Dewilde, S., Green, B. N., Pesce, A., Uzan, J., Burmester, T., Hankeln, T., Bolognesi, M., Moens, L. and Marden, M. C. (2004) Coupling of the heme and an internal disulfide bond in human neuroglobin. Micron **35**, 59–62
9 Hamdane, D., Kiger, L., Dewilde, S., Green, B. N., Pesce, A., Uzan, J., Burmester, T., Hankeln, T., Bolognesi, M., Moens, L. and Marden, M. C. (2003) The redox state of the cell regulates the ligand binding affinity of human neuroglobin and cytoglobin. J. Biol. Chem. **278**, 51713–51721
10 Pesce, A., Dewilde, S., Nardini, M., Moens, L., Ascenzi, P., Hankeln, T., Burmester, T. and Bolognesi, M. (2003) Human brain neuroglobin structure reveals a distinct mode of controlling oxygen affinity. Structure **11**, 1087–1095
11 Smagghe, B. J., Sarath, G., Ross, E., Hilbert, J-L. and Hargrove, M. S. (2006) Slow ligand binding kinetics dominate ferrous hexacoordinate hemoglobin reactivities and reveal differences between plants and other species. Biochemistry **45**, 561–570
12 Fago, A., Hundahl, C., Dewilde, S., Gilany, K., Moens, L. and Weber, R. E. (2004) Allosteric regulation and temperature dependence of oxygen binding in human neuroglobin and cytoglobin. Molecular mechanisms and physiological significance. J. Biol. Chem. **279**, 44417–44426
13 Pesce, A., Dewilde, S., Nardini, M., Moens, L., Ascenzi, P., Hankeln, T., Burmester, T. and Bolognesi, M. (2004) The human brain hexacoordinated neuroglobin three-dimensional structure. Micron **35**, 63–65
14 Vallone, B., Nienhaus, K., Matthes, A., Brunori, M. and Nienhaus, G. U. (2004) The structure of carbonmonoxy neuroglobin reveals a heme-sliding mechanism for control of ligand affinity. Proc. Natl. Acad. Sci. U.S.A. **101**, 17351–17356
15 Brunori, M., Giuffrè, A., Nienhaus, K., Nienhaus, G. U., Scandurra, F. M. and Vallone, B. (2005) Neuroglobin, nitric oxide, and oxygen: functional pathways and conformational changes. Proc. Natl. Acad. Sci. U.S.A. **102**, 8483–8488
16 Sun, Y., Jin, K., Peel, A., Mao, X. O., Xie, L. and Greenberg, D. A. (2003) Neuroglobin protects the brain from experimental stroke *in vivo*. Proc. Natl. Acad. Sci. U.S.A. **100**, 3497–3500
17 Sun, Y., Jin, K., Mao, X. O., Zhu, Y. and Greenberg, D. A. (2001) Neuroglobin is up-regulated by and protects neurons from hypoxic-ischemic injury. Proc. Natl. Acad. Sci. U.S.A. **98**, 15306–15311
18 Lipton, P. (1999) Ischemic cell death in brain neurons. Physiol. Rev. **79**, 1431–1568
19 Herold, S., Fago, A., Weber, R. E., Dewilde, S. and Moens, L. (2004) Reactivity studies of the Fe^{III} and $Fe^{II}NO$ forms of human neuroglobin reveal a potential role against oxidative stress. J. Biol. Chem. **279**, 22841–22847
20 Herold, S. and Fago, A. (2005) Reactions of peroxynitrite with globin proteins and their possible physiological role. Comp. Biochem. Physiol. A: Mol. Integr. Physiol. **142**, 124–129
21 Van der Vliet, A., Eiserich, J. P., Halliwell, B. and Cross, C. E. (1997) Formation of reactive nitrogen species during peroxidase-catalyzed oxidation of nitrite. A potential additional mechanism of nitric oxide-dependent toxicity. J. Biol. Chem. **272**, 7617–7625
22 Monzani, E., Roncone, R., Casella, L., Galliano, M. and Koppenol, W. H. (2004) Mechanistic insight into the peroxidase catalyzed nitration of tyrosine derivatives by nitrite and hydrogen peroxide. Eur. J. Biochem. **271**, 895–906
23 Nicolis, S., Monzani, E., Roncone, R., Gianelli, L. and Casella, L. (2004) Metmyoglobin-catalyzed exogenous and endogenous tyrosine nitration by nitrite and hydrogen peroxide. Chem. Eur. J. **10**, 2281–2290
24 Nicolis, S., Pennati, A., Perani, E., Monzani, E., Sanangelantoni, A. M. and Casella, L. (2006) Easy oxidation and nitration of human myoglobin by nitrite and hydrogen peroxide. Chem. Eur. J. **12**, 749–757
25 Sacksteder, C. A., Qian, W-J., Knyushko, T. V., Wang, H., Chin, M. H., Lacan, G., Melega, W. P., Camp, II, D. G., Smith, R. D., Smith, D. J. et al. (2006) Endogenously nitrated proteins in mouse brain: links to neurodegenerative disease. Biochemistry **45**, 8009–8022
26 Turko, I. V. and Murad, F. (2002) Protein nitration in cardiovascular diseases. Pharmacol. Rev. **54**, 619–634
27 Hunt, J., Byrns, R. E., Ignarro, L. J. and Gaston, B. (1995) Condensed expirate nitrite as a home marker for acute asthma. Lancet **346**, 1235–1236
28 Torre, D., Ferrario, G., Speranza, F., Orani, A., Fiori, G. P. and Zeroli, C. (1996) Serum concentrations of nitrite in patients with HIV-1 infection. J. Clin. Pathol. **49**, 574–576

29 Pryor, W. A. and Squadrito, G. L. (1995) The chemistry of peroxynitrite: a product from the reaction of nitric oxide with superoxide. Am. J. Physiol. **268**, L699–L722
30 Casella, L., De Gioia, L., Frontoso Silvestri, G., Monzani, E., Redaelli, C., Roncone, R. and Santagostini, L. (2000) Covalently modified microperoxidases as heme-peptide models for peroxidases. J. Inorg. Biochem. **79**, 31–39
31 Antonini, E. and Brunori, M. (1971) Hemoglobin and Myoglobin in Their Reactions with Ligands, North-Holland Publishing Company, Amsterdam
32 Roncone, R., Monzani, E., Labò, S., Sanangelantoni, A. M. and Casella, L. (2005) Catalytic activity, stability, unfolding, and degradation pathways of engineered and reconstituted myoglobins. J. Biol. Inorg. Chem. **10**, 11–24
33 Fuhrhop, J. H. and Smith, K. M. (1975) Laboratory Methods In Porphyrin And Metalloporphyrin Research, Elsevier, Amsterdam
34 Grassetti, D. R. and Murray, J. F. (1967) Determination of sulfhydryl groups with 2,2′- or 4,4′-dithiodipyridine. Arch. Biochem. Biophys. **119**, 41–49
35 Hogg, P. J. (2003) Disulfide bonds as switches for protein function. Trends Biochem. Sci. **28**, 210–214
36 Du, W., Syvitski, R., Dewilde, S., Moens, L. and La Mar, G. N. (2003) Solution ^{1}H NMR characterization of equilibrium heme orientational disorder with functional consequences in mouse neuroglobin. J. Am. Chem. Soc. **125**, 8080–8081
37 Nistor, S. V., Goovaerts, E., Van Doorslaer, S., Dewilde, S. and Moens, L. (2002) EPR-spectroscopic evidence of a dominant His-Fe^{III}-His coordination in ferric neuroglobin. Chem. Phys. Lett. **361**, 355–361
38 Watanabe, Y. and Ueno, T. (2003) Introduction of P450, peroxidase, and catalase activities into myoglobin by site-directed mutagenesis: diverse reactivities of compound I. Bull. Chem. Soc. Jpn. **76**, 1309–1322
39 Roncone, R., Monzani, E., Nicolis, S. and Casella, L. (2004) Engineering and prosthetic group modification of myoglobin: peroxidase activity, chemical stability and unfolding properties, Eur. J. Inorg. Chem., 2203–2213
40 Hayashi, T., Hitomi, Y., Ando, T., Mizutani, T., Hisaeda, Y., Kitagawa, S. and Ogoshi, H. (1999) Peroxidase activity of myoglobin is enhanced by chemical mutation of heme-propionates. J. Am. Chem. Soc. **121**, 7747–7750
41 Dunford, H. B. (1999) Heme Peroxidases, Wiley-VCH, New York
42 Monzani, E., Gatti, A. L., Profumo, A., Casella, L. and Gullotti, M. (1997) Oxidation of phenolic compounds by lactoperoxidase. Evidence for the presence of a low-potential compound II during catalytic turnover. Biochemistry **36**, 1918–1926
43 Sampson, J. B., Ye, Y. Z., Rosen, H. and Beckman, J. S. (1998) Myeloperoxidase and horseradish peroxidase catalyze tyrosine nitration in proteins from nitrite and hydrogen peroxide. Arch. Biochem. Biophys. **356**, 207–213
44 Eiserich, J. P., Hristova, M., Cross, C. E., Jones, A. D., Freeman, B. A., Halliwell, B. and van der Vliet, A. (1998) Formation of nitric oxide-derived inflammatory oxidants by myeloperoxidase in neutrophils. Nature **391**, 393–397
45 Herold, S. and Rehmann, F. J. (2001) Kinetic and mechanistic studies of the reactions of nitrogen monoxide and nitrite with ferryl myoglobin. J. Biol. Inorg. Chem. **6**, 543–555
46 Casella, L., Monzani, E., Roncone, R., Nicolis, S., Sala, A. and De Riso, A. (2002) Formation of reactive nitrogen species at biologic heme centers: a potential mechanism of nitric oxide-dependent toxicity. Environ. Health Perspect. **110**, 709–711
47 Bondoc, L. L. and Timkovich, R. (1989) Structural characterization of nitrimyoglobin. J. Biol. Chem. **264**, 6134–6145
48 Fago, A., Mathews, A. J., Dewilde, S., Moens, L. and Brittain, T. (2006) The reactions of neuroglobin with CO: evidence for two forms of the ferrous protein. J. Inorg. Biochem. **100**, 1339–1343
49 Radi, R., Beckman, J. S., Bush, K. M. and Freeman, B. A. (1991) Peroxynitrite oxidation of sulfhydryls. The cytotoxic potential of superoxide and nitric oxide. J. Biol. Chem. **266**, 4244–4250
50 Hamann, M., Zhang, T., Hendrich, S. and Thomas, J. A. (2002) Quantitation of protein sulfinic and sulfonic acid, irreversibly oxidized protein cysteine sites in cellular proteins. Methods Enzymol. **348**, 146–156
51 Woo, H. A., Jeong, W., Chang, T.-S., Park, K. J., Park, S. J., Yang, J. S. and Rhee, S. G. (2005) Reduction of cysteine sulfinic acid by sulfiredoxin is specific to 2-Cys peroxiredoxins. J. Biol. Chem. **280**, 3125–3128
52 Jacob, C., Holme, A. L. and Fry, F. H. (2004) The sulfinic acid switch in proteins. Org. Biomol. Chem. **2**, 1953–1956

Received 16 March 2007/24 May 2007; accepted 29 June 2007
Published as BJ Immediate Publication 29 June 2007, doi:10.1042/BJ20070372